

---

# BENCHMARKING 3D HUMAN POSE ESTIMATION MODELS UNDER OCCLUSIONS

---

**Filipa Lino, Carlos Santiago, Manuel Marques**

Institute for Systems and Robotics, LARSyS

Instituto Superior Técnico

Portugal

{filipa.lino, carlos.santiago}@tecnico.ulisboa.pt, manuel@isr.tecnico.ulisboa.pt

## ABSTRACT

This paper addresses critical challenges in 3D Human Pose Estimation (HPE) by analyzing the robustness and sensitivity of existing models to occlusions, camera position, and action variability. Using a novel synthetic dataset, BlendMimic3D, which includes diverse scenarios with multi-camera setups and several occlusion types, we conduct specific tests on several state-of-the-art models. Our study focuses on the discrepancy in keypoint formats between common datasets such as Human3.6M, and 2D datasets such as COCO, commonly used for 2D detection models and frequently input of 3D HPE models. Our work explores the impact of occlusions on model performance and the generality of models trained exclusively under standard conditions. The findings suggest significant sensitivity to occlusions and camera settings, revealing a need for models that better adapt to real-world variability and occlusion scenarios. This research contributed to ongoing efforts to improve the fidelity and applicability of 3D HPE systems in complex environments.

**Keywords** 3D Human Pose Estimation · Occlusions · 2D Detections · Human3.6M Dataset · BlendMimic3D Dataset

## 1 Introduction

Human Pose Estimation (HPE) presents a significant challenge in computer vision, impacting a wide range of applications, from healthcare, sports to retail or human-machine interaction. 3D Human Pose Estimation (HPE) involves predicting the 3D coordinates of each keypoint in a skeleton, based on a person detected from images or videos. Over the years, various models [1–9] have been developed to address this challenge, with a significant focus on the method of lifting from 2D to 3D poses. This approach generally yields superior performance compared to direct 3D pose prediction from images, mainly because 2D HPE currently achieves state-of-the-art results. Given these developments, our focus shifts to practical applications: How effectively can these models perform in real-world scenarios? To address this, we evaluate several state-of-the-art models for which code and pre-trained models are available [1–9].

In practical applications, two-stage models first capture a person on camera, detect 2D keypoints, and then lift them to a 3D pose. However, occlusions—whether self-imposed by objects, the frame’s edge, or by overlapping in multi-person scenarios—can lead to inaccuracies in detected 2D poses. Our research thus focuses on how well lifting models can handle these inaccuracies: Can they effectively predict 3D poses from noisy 2D inputs?

Most existing studies use the Human3.6M [10] dataset, which is a controlled environment with indoor settings and minimal obstructions, except for occasional objects in scenarios such as sitting poses. This setup does not fully represent the challenges of real-world occlusions. We opt for the BlendMimic3D [11] dataset, which includes occlusion labels and synthetic images with occlusions, allowing us to specifically assess model performance under varying occlusion conditions. A challenge we faced was the disparity in keypoint formats across datasets [10–12]. Thus, we had to adjust the BlendMimic3D format to align it as closely as possible with Human3.6M, thereby facilitating the testing of state-of-the-art (SOTA) models.

This paper raises questions about the applicability of recent 3D HPE advances to real-world settings and the adequacy of current benchmarks. We performed several tests and analysis on different models to evaluate the strengths and

weaknesses of each mode. We analyze their behavior under occlusion, and study the impact of the training set on model robustness and generalizability.

## 2 Related Work

In Human Pose Estimation (HPE), deep learning has significantly enhanced the 2D pose estimation. However, the same level of progress has not been achieved for 3D HPE due to depth ambiguities, insufficient training data, and occlusions [13]. Enhancing 3D HPE is crucial for applications such as healthcare, where it supports patient monitoring and physical therapy, in sports for performance analysis and injury prevention, and in retail to optimize customer service and security. These real-world applications demand robust pose estimation that can handle occlusions effectively.

In monocular images, 3D HPE is typically divided into: direct estimation and 2D-to-3D lifting. Direct methods infer 3D poses without intermediately predicting 2D poses. [14] proposed a dual-branch network leveraging body part correlations. [15] addressed depth ambiguities during training using voxel-wise joint likelihoods. [16] addressed the challenge of merging training data from different datasets, which use inconsistent skeleton formats (i.e., label different anatomical landmarks), by introducing a latent keypoint set as an intermediate representation to unify the data for model training. However, direct-based methods may struggle to resolve ambiguities, such as occlusions, due to limited depth and contextual cues.

Many studies have adopted 2D-to-3D lifting approaches, benefiting from the advances in 2D HPE. Temporal information was incorporated [17] to address video sequences, however, it assumes independence between consecutive errors. Graph-based approaches [18, 19] have been applied to model relationships between keypoints over time. Also, transformer architectures [20, 21] process spatial-temporal features with attention mechanisms, leading to more robust 3D HPE. Diffusion-based approaches [22, 23] generate and refine multiple 3D pose hypotheses from 2D observations by gradually denoising sampled data. Nonetheless, the accuracy of these methods heavily rely on the quality of 2D inputs. In 2D detection, some keypoints are more easily detectable than others due to their scale [24], and 3D HPE models typically allocate equal attention to all keypoints, yet, we show that as the degrees of freedom increase, so does the estimation complexity per keypoint.

Our work [11] employed graph-based 3D pose refinement block trained on occluded scenarios. While effective in these conditions, this approach does not consistently perform well in non-occluded settings, highlighting the need for occlusion-aware networks. Addressing this, [25] included a cylinder man model to generate self-occlusion labels. [9] introduced an occlusion guidance mechanism that estimates missing joints, yet limited by the assumption of pre-existing occlusion detection models. [26] separates features into occlusion-aware and view-dependent components, completing occluded poses in 2D space, potentially leading to inaccurate 3D coordinates. [27] reconstructs occluded parts in 3D but does not address all occlusion types. Thus, there is still room for improvement in occlusion-aware models. Despite the advancements in 3D HPE [13], there remains a need for methods that can handle occlusions under complex conditions. This proposed work aims to address these gaps by identifying outliers in the 3D pose prediction process, leveraging variations in human keypoints, exploring viable pose spaces, and tackling the challenge of merging different dataset formats. Additionally, our BlendMimic3D dataset [11], enriched with occlusion labels, enables targeted evaluation of occlusion-handling performance.

Working on multiple datasets with different skeleton annotations [16, 28], even though they sometimes share the same joint names. For example, the hip keypoints are at different heights, some body parts are only labeled in some datasets, some provide surface markers while others provide keypoints inside the body, etc. The AMASS dataset [29] addresses the problem of discrepancy in MoCap data representations by mapping them to the SMPL [30] representation, a widely used body model that defines the 3D mesh of a human body, however our work is to predict 3D skeletons and not mesh. In our research context, 2D-to-3D pose lifting [28] combine pairs of datasets in training by concatenating the training data sets, and harmonize the joints through hand-crafted rules (e.g., shrink the hip-pelvis distance by a certain factor), but this does not scale to many keypoints and datasets. [16] approached this problem with an autoencoder-based dimensionality reduction model to compress the 3D keypoints from all datasets into a smaller latent keypoint set. However, they did not generated a definitive, universal ground truth representation for all datasets, their latent keypoint set is used as an intermediate representation for their pose estimation.

## 3 Methodology

The simulation of real-world conditions in our keypoints dataset involves introducing Gaussian noise to model inaccuracies typically generated by 2D HPE detectors under occlusions. In order to maintain consistency across different sizes of input images, the noise level is based on the frame resolution. The standard deviation of the noise,  $\sigma$  is

Table 1: Study on the error of 2D HPE detectors under occluded keypoints on BlendMimic3D dataset. The metric presented is MPJPE (pixel) on 1000x1002 images.

	CPN [31]		Detectron2 [32]	
	Mean	Std	Mean	Std
<b>Visible Keypoints</b>	75.60	0.015	75.50	0.015
<b>Occluded Keypoints</b>	59.09	0.023	56.77	0.023
<b>All Visible</b>	—	—	—	—
<b>All Occluded</b>	111.70	0.048	120.57	0.036

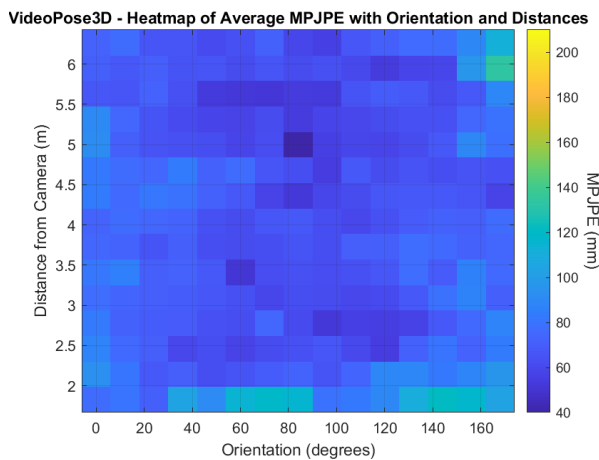


Figure 1: VideoPose3D performance heatmap. Average MPJPE with pose orientation and distances from pose to camera.

computed as follows

$$\sigma = \text{noise\_level} \times \text{mean}(res_w, res_h) \quad (1)$$

where `noise_level` is a predefined constant that scales the noise intensity, and `res_w` and `res_h` are the width and height of the frame, respectively. We considered `noise_level = {0, 0.001, 0.005, 0.01, 0.03, 0.05}`, this means that if `noise_level = 0`, no noise is added to the keypoints, that is, the 2D ground truth will be used.

## 4 Experiments

### 4.1 Camera-Related Sensitivity

The analysis here is done in two different ways: the placement and distance of camera, we wanted to evaluate each model performance as a function of camera distance from the subject. So we firstly used the 2D poses from Blendimic3D, projected from 3D ground truth and so, without any occlusion.

Fig. 1 shows that the MPJPE decreases as the distance from the camera increases. This could suggest that closer distances present more challenges in accurately estimation the pose, possibly due to larger variations in scale. The model was trained under 2D detections, that is, with errors related to occlusions. This might explain the unexpected behavior of higher MPJPE on front and back poses and not side ones (which in training setting has self-occlusions). The highest errors occur at closer distances with specific challenging orientations - this might be related to the training data distribution.

We checked the distribution of poses under orientation and distance of both BlendMimic3D (testing data) and Human3.6M (training data), shown in Fig. 2. As we can see, the model didn't see, while training, distances below 2.5 m, explaining why the highest MPJPE on closer and unseen distances. Therefore the model doesn't generalize that well to new types of data. However, this doesn't explain the highest MPJPE on biggest orientation bins and distance between 5.5 and 6.5, the model could've had worst performance on that criteria even on training data, the poses itself could be difficult, the movement fast, etc..

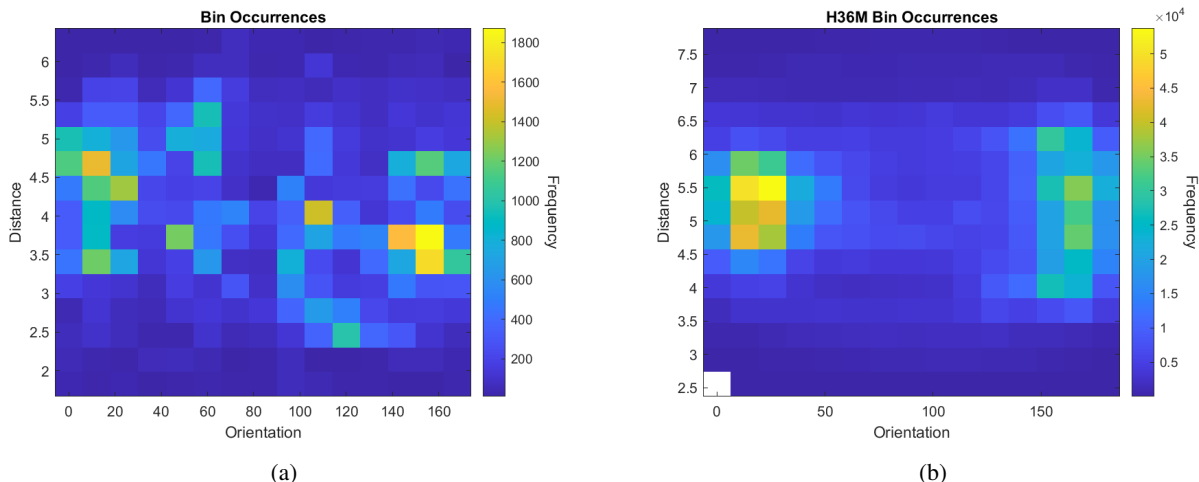


Figure 2: Heatmaps of the distribution of data, the frequency related to orientation of poses and distances from poses to camera in (a) BlendMimic3D dataset and (b) Human3.6M dataset.

Comparison of 2D Human Poses at Different Noise Levels

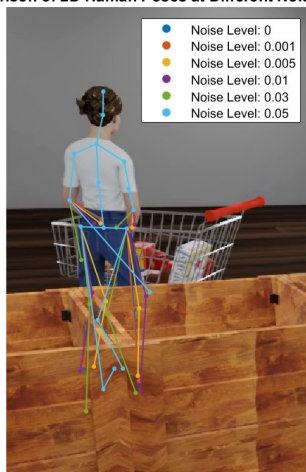


Figure 3: 2D human poses from the ground truth skeleton with different noise levels.

## 4.2 Occlusion Handling

In this part of the study, we have employed a systematic approach to evaluate the performance of pose estimation models under conditions of occluded keypoints. Each model, pretrained on the Human3.6M dataset and with CPN 2D detections, was tested against a simulated occlusion environment. This simulation was achieved by injecting Gaussian noise into the 2D ground truth poses from the BlendMimic3D dataset, a process repeated across various predefined noise levels (sigma levels from 0 to 0.05) in multiple runs (10 runs per sigma level).

The purpose of this methodology is to understand how well each model can infer 3D poses from corrupted 2D input data, a critical measure of robustness in real-world applications where occlusions are common. By tracking the performance degradation across different noise intensities, we can assess the models’ capacity to handle partial visibility of keypoints, thus providing insights into their practical usability in occlusion-heavy scenarios.

To simulate occlusions in 3D pose estimation, we conducted tests by introducing Gaussian noise to 2D ground truth poses as seen in Fig. 3. Using the BlendMimic3D dataset, we experimented with various noise levels, defined by sigma levels ranging from 0 to 0.05 across five experimental runs. For each test, we loaded occlusion labels and adjusted the 2D poses accordingly. Specifically, the noise intensity was dynamically adjusted based on the resolution of the

## Benchmarking 3D Human Pose Estimation Models Under Occlusions

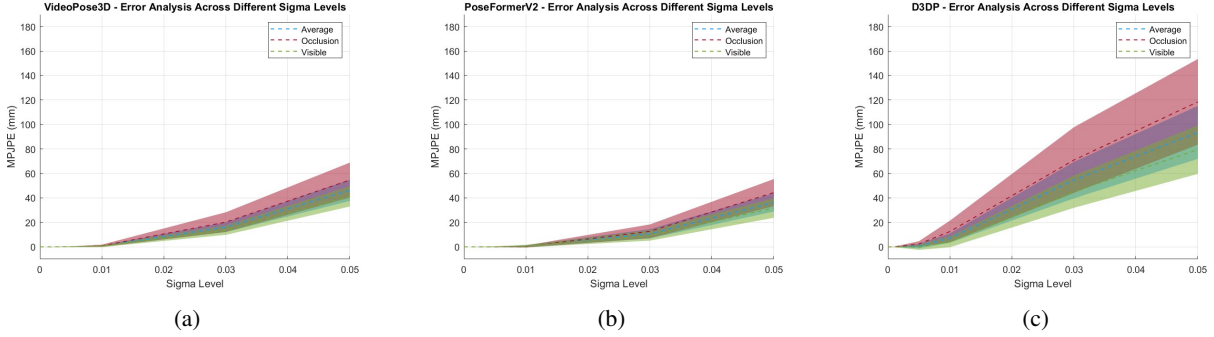


Figure 4: MPJPE across different noise levels, normalized by the ground truth based results per model, (a) VideoPose3D, (b) PoseFormerV2 and (c) D3DP.

Table 2: Evaluation of 3D HPE of state-of-the-art models under several levels of simulated occlusion noise on BlendMimic3D. The metric presented is MPJPE (mm). The best results for each noise level are highlighted in **bold**.

Models	Year	Noise Level					
		$\sigma = 0$	$\sigma = 0.001$	$\sigma = 0.005$	$\sigma = 0.01$	$\sigma = 0.03$	$\sigma = 0.05$
VideoPose3D [1]	2019	69.59 ± 4.57	69.59 ± 4.42	69.73 ± 4.42	70.37 ± 4.46	85.75 ± 4.61	115.88 ± 7.52
P-STMO [2]	2022	71.00 ± 4.39	70.98 ± 4.25	70.55 ± 4.40	70.61 ± 4.64	107.84 ± 6.93	150.98 ± 9.29
MixSTE [3]	2022	<b>65.37 ± 4.34</b>	<b>65.42 ± 4.24</b>	67.54 ± 4.76	74.61 ± 6.29	124.18 ± 13.37	164.90 ± 16.03
PoseFormerV2 [4]	2023	68.90 ± 3.98	68.90 ± 3.86	68.98 ± 3.99	<b>69.46 ± 4.39</b>	<b>79.60 ± 5.63</b>	105.28 ± 7.79
D3DP [5]	2023	65.73 ± 3.52	65.70 ± 3.40	<b>66.41 ± 3.99</b>	72.9 ± 5.62	120.31 ± 15.81	159.33 ± 22.19
DiffuPose [6]	2023	78.96 ± 6.54	79.16 ± 6.29	83.70 ± 6.25	95.72 ± 6.53	159.59 ± 11.93	211.48 ± 15.68
FinePose [7]	2024	65.64 ± 8.34	65.67 ± 8.14	66.62 ± 9.10	72.79 ± 10.46	125.23 ± 17.73	173.05 ± 22.54
DTF [9]	2024	76.07 ± 3.47	87.89 ± 3.69	87.89 ± 3.74	87.96 ± 3.79	88.61 ± 4.03	<b>90.11 ± 4.56</b>

camera frame from which the 2D poses were derived. Occluded keypoints were identified using the occlusion labels, and Gaussian noise, scaled by the calculated sigma, was applied only to these occluded keypoints. This approach allowed for a controlled simulation of occlusions, facilitating a detailed analysis of each model’s robustness to noise under different conditions. So, here we have the labels of the actual occlusions per keypoint in the BlendMimic3D dataset, we simply adjust the deviation of each occluded keypoint.

## 5 Results and Discussion

### 5.1 Occlusion Handling

We compare each model performance per sigma level and check the MPJPE, mean and standard deviation over all runs and in 3 different ways. We check the average MPJPE, that is, the error per pose, the error only on occluded keypoints per pose and of the visible keypoints per pose. As we can see, in every model the occluded keypoints start with a small MPJPE and this is related to the easiness of some specific keypoints (to be seen). We normalized the previous 3 plots to the increase of MPJPE to the case without occlusions, that is with sigma = 0, to check how much does the MPJPE increase with sigma.

While D3DP presents the best performance in SOTA compared to PFV2 and VP3D, with Fig. 4 here we prove that, in fact D3DP has the best performance but only with small or no occlusions, with sigma higher than 0.01 D3DP presents worst performance as sigma increases.

Table 2 presents the evaluation of several state-of-the-art 3D Human Pose Estimation (HPE) models under increasing levels of simulated occlusion noise on the BlendMimic3D dataset. The reported metric is MPJPE (Mean Per Joint Position Error) in millimeters, with lower values indicating better performance.

At zero noise ( $\sigma = 0$ ), MixSTE achieves the best performance (65.37 mm), closely followed by FinePose (65.64 mm) and D3DP (65.73 mm). As noise increases slightly ( $\sigma = 0.001$  and  $\sigma = 0.005$ ), MixSTE and D3DP alternate in securing the best results, with D3DP marginally outperforming at  $\sigma = 0.005$ .

At moderate noise levels ( $\sigma = 0.01$  and  $\sigma = 0.03$ ), PoseFormerV2 shows strong robustness, outperforming others with MPJPE values of 69.46 mm and 79.60 mm respectively. This indicates PoseFormerV2’s relatively higher resilience to medium levels of occlusion noise compared to more traditional models like VideoPose3D or newer diffusion-based approaches like DiffuPose.

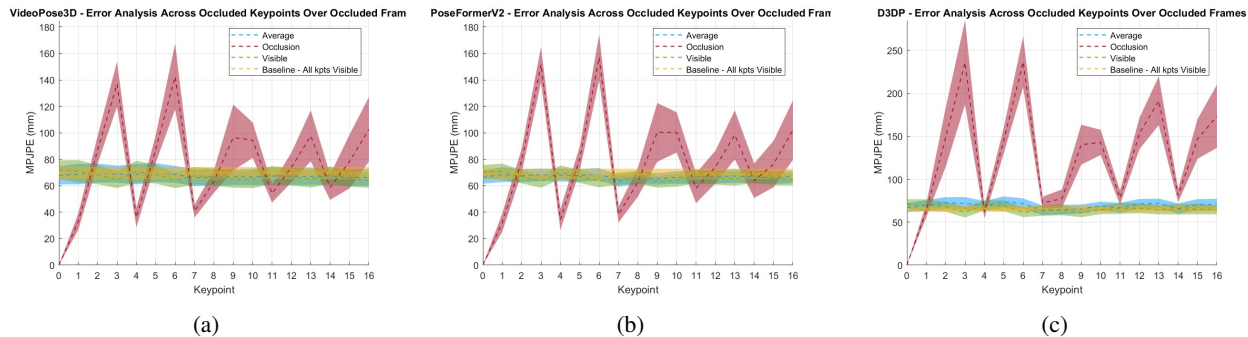


Figure 5: MPJPE per occluded keypoints (simulated noise) per model, (a) VideoPose3D, (b) PoseFormerV2 and (c) D3DP.

At the highest noise level ( $\sigma = 0.05$ ), an interesting trend emerges: DTF achieves the lowest MPJPE (90.11 mm), outperforming all other models. While DTF performs worse at lower noise levels, its performance degrades significantly less as noise increases, suggesting that DTF may be particularly well-suited for highly corrupted inputs.

Models like DiffuPose show considerable sensitivity to noise, with a consistent degradation leading to the worst performance across all noise levels. Despite being a recent method, DiffuPose’s higher MPJPE values highlight potential challenges for diffusion-based models under noisy conditions.

Overall, the results illustrate that while some models (e.g., MixSTE, D3DP, PoseFormerV2) maintain strong performance in low-to-moderate noise, others like DTF may offer better robustness under extreme occlusions. These findings underscore the importance of evaluating 3D HPE models not only on clean data but also under challenging, real-world-like scenarios involving partial occlusions.

In the second part of the study, and based on the detector error analysis, a sigma level of 0.03 was selected for further tests. This level was chosen as it likely represents a reasonable compromise for occlusion conditions, offering a practical level of noise for simulating real-world scenarios in further tests.

To implement this, noise was added to the 2D keypoints to simulate occlusion, affecting only the selected keypoint during the specified frames. This approach allows for a detailed analysis of each keypoint’s contribution to the overall pose accuracy, helping to identify which keypoints are critical for maintaining high performance in pose estimation models. By systematically altering each keypoint in turn, the test offered a comprehensive view of the importance of each part of the body in the 3D reconstruction process, highlighting potential weaknesses in the models’ abilities to infer occluded parts.

With the results presented in Fig. 5 we detected a pattern on the occluded keypoints: some are easier to estimate than others. So we also checked if this behavior is still noticeable without occlusions.

We also study how much worse each keypoint gets when occluded. For that, following Fig. 6

From Fig. 6, in the difference in MPJPE of VideoPose3D and PoseFormerV2 we saw some negative values, that is, in some of the considered “easy to estimate” keypoints their averaged MPJPE got better when occluded. However this difference is not considerable and does not affect that much.

We also checked if this behavior is also visible in the real case, with the actual occlusions and not with the forced one by one occluded keypoint. We checked the error of each keypoint in the cases with the real groups of occlusion labels versus the error of each keypoint from the frames where that keypoint is visible, presented in Fig. 7. Thus, we can conclude that, in fact, some keypoints are easier to estimate than others: keypoint 0 (pelvis), 1, 4 (hips), 7 (spine), 8 (neck), 11, 14 (shoulders). And, the keypoints with higher degree of freedom: 2, 5 (knees), 3, 6 (feet), 9 (nose), 10 (head), 12, 15 (elbows), 13, 16 (hands), are related to the highest MPJPE.

## 6 Challenges and Limitations

Throughout this study, several important challenges and limitations of current 3D Human Pose Estimation (HPE) models became evident. One of the main issues encountered was the incompatibility between skeleton formats across datasets. While most 3D HPE models are trained using the Human3.6M keypoint format, real-world 2D detectors often

## Benchmarking 3D Human Pose Estimation Models Under Occlusions

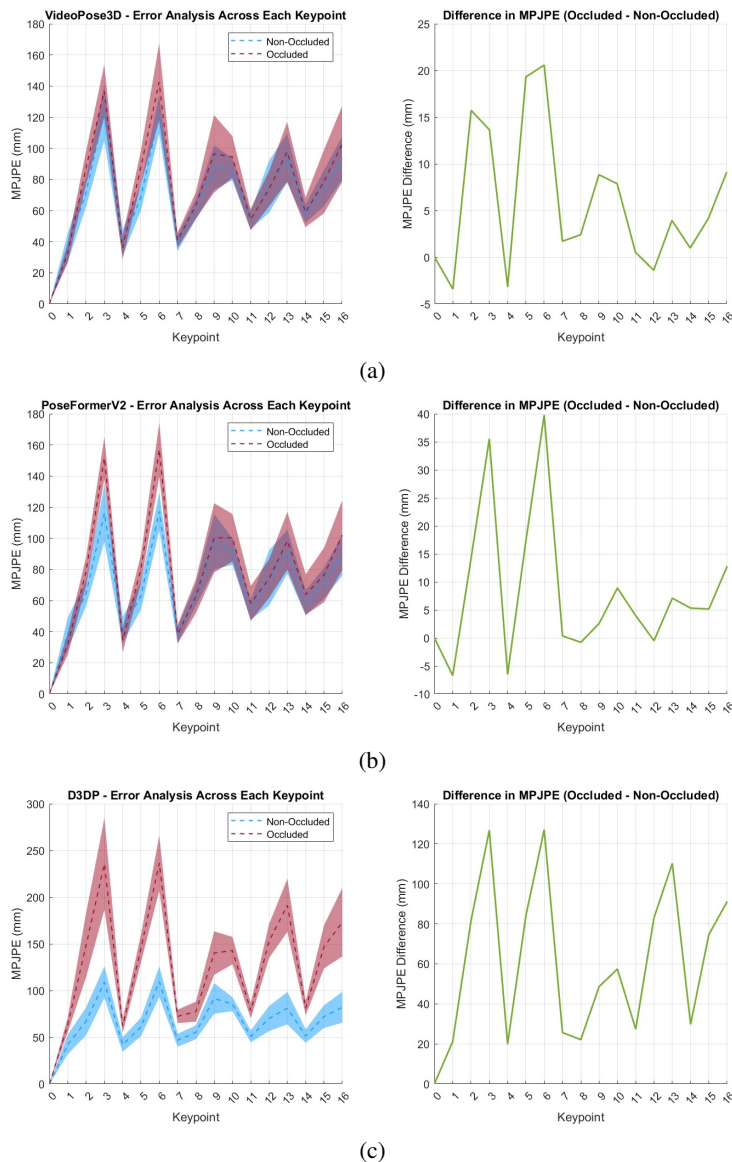


Figure 6: MPJPE per keypoint occluded, with simulated noise, versus visible and MPJPE differences between them per model, (a) VideoPose3D, (b) PoseFormerV2 and (c) D3DP.

output keypoints based on the COCO format. This mismatch introduces additional errors unless a careful alignment and mapping are performed between the two formats.

Another significant challenge relates to the sensitivity of models to camera distance and orientation. Models trained exclusively on Human3.6M struggle when evaluated under camera distances or viewing angles that were not present during training, particularly at closer distances and in extreme side-view poses. This reveals a clear gap in the generalization ability of current approaches.

Handling occlusions also remains a major difficulty. Most state-of-the-art models suffer a noticeable drop in performance when keypoints are partially or fully occluded. In particular, models like D3DP, despite showing strong results under clean conditions, tend to degrade rapidly as occlusion levels increase. This indicates that robustness to missing or corrupted input remains an open challenge in 3D HPE.

Limitations were also observed in the simulation of noise to replicate real-world occlusion conditions. Applying a fixed noise level across all frames does not perfectly reflect the behavior of actual 2D detectors, whose performance varies

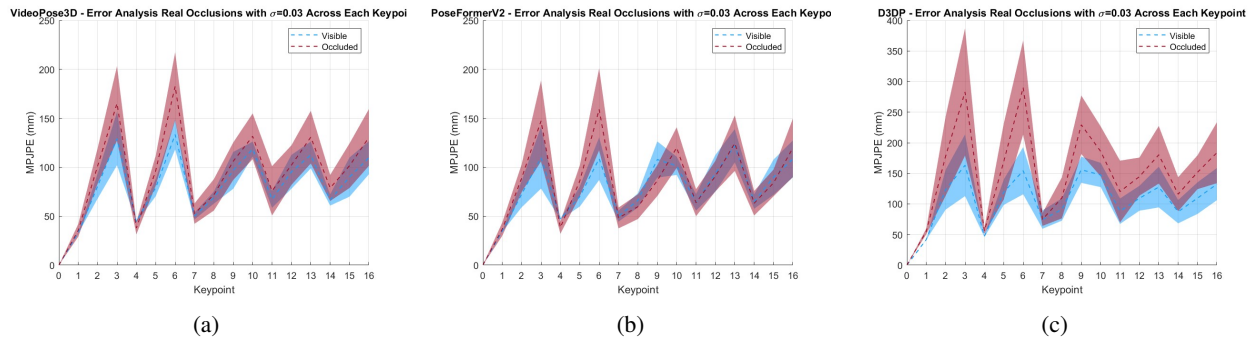


Figure 7: MPJPE per keypoint occluded, with simulated noise, in the actual BlendMimic3D occlusions, versus visible and MPJPE differences between them per model, (a) VideoPose3D, (b) PoseFormerV2 and (c) D3DP.

depending on the distance to the camera and the pose orientation. As a result, noise simulation may introduce artifacts that do not accurately mirror real-world challenges.

Finally, the dependency of model performance on specific keypoints was apparent. Keypoints with greater freedom of movement, such as the hands, feet, and head, consistently resulted in higher errors, especially when occluded. This suggests an intrinsic difficulty for models to reliably predict the more flexible and dynamic parts of the human body.

Taken together, these findings highlight that despite strong performances reported on benchmark datasets, current state-of-the-art 3D HPE models are not yet fully robust for real-world applications, especially in scenarios involving diverse camera setups, significant occlusions, and dynamic poses.

## 7 Conclusion

In this paper, we analyzed the sensitivity and robustness of leading 3D Human Pose Estimation models under realistic conditions, focusing on camera placement, action variability, and occlusions.

By using the BlendMimic3D dataset with synthetic occlusions and carefully aligning keypoint formats, we showed that current models are highly sensitive to factors not well represented in their training data. Models generally perform well under ideal conditions but face difficulties under occlusions, unseen camera distances, and rapid motion. Notably, model robustness varies: while some models like D3DP perform well under low-noise conditions, they degrade faster than others when faced with higher occlusion levels.

Our work emphasizes the need for more diverse and realistic training datasets, better handling of noisy or partial 2D detections, tools to standardize keypoint formats across datasets, new model designs that are less sensitive to occlusion and camera variations.

Future research should focus on improving generalization, especially towards real-world environments where perfect visibility of poses cannot be guaranteed. BlendMimic3D, as introduced here, can serve as a valuable resource for benchmarking and advancing 3D HPE models in these more challenging scenarios.

## References

- [1] Dario Pavlo, Christoph Feichtenhofer, David Grangier, and Michael Auli. 3d human pose estimation in video with temporal convolutions and semi-supervised training. In *Proceedings of the IEEE/CVF conference on computer vision and pattern recognition*, pages 7753–7762, 2019.
- [2] Wenkang Shan, Zhenhua Liu, Xinfeng Zhang, Shanshe Wang, Siwei Ma, and Wen Gao. P-stmo: Pre-trained spatial temporal many-to-one model for 3d human pose estimation. In *European Conference on Computer Vision*, pages 461–478. Springer, 2022.
- [3] Jinlu Zhang, Zhigang Tu, Jianyu Yang, Yujin Chen, and Junsong Yuan. Mixste: Seq2seq mixed spatio-temporal encoder for 3d human pose estimation in video. In *Proceedings of the IEEE/CVF conference on computer vision and pattern recognition*, pages 13232–13242, 2022.

- [4] Qitao Zhao, Ce Zheng, Mengyuan Liu, Pichao Wang, and Chen Chen. Poseformerv2: Exploring frequency domain for efficient and robust 3d human pose estimation. In *Proceedings of the IEEE/CVF conference on computer vision and pattern recognition*, pages 8877–8886, 2023.
- [5] Wenkang Shan, Zhenhua Liu, Xinfeng Zhang, Zhao Wang, Kai Han, Shanshe Wang, Siwei Ma, and Wen Gao. Diffusion-based 3d human pose estimation with multi-hypothesis aggregation. In *Proceedings of the IEEE/CVF International Conference on Computer Vision*, pages 14761–14771, 2023.
- [6] Jeongjun Choi, Dongseok Shim, and H Jin Kim. Diffupose: Monocular 3d human pose estimation via denoising diffusion probabilistic model. In *2023 IEEE/RSJ International Conference on Intelligent Robots and Systems (IROS)*, pages 3773–3780. IEEE, 2023.
- [7] Jinglin Xu, Yijie Guo, and Yuxin Peng. Finepose: Fine-grained prompt-driven 3d human pose estimation via diffusion models. In *Proceedings of the IEEE/CVF Conference on Computer Vision and Pattern Recognition*, pages 561–570, 2024.
- [8] Mehwish Ghafoor and Arif Mahmood. Quantification of occlusion handling capability of a 3d human pose estimation framework. *IEEE Transactions on Multimedia*, 25:3311–3318, 2022.
- [9] Mehwish Ghafoor, Arif Mahmood, and Muhammad Bilal. Enhancing 3d human pose estimation amidst severe occlusion with dual transformer fusion. *IEEE Transactions on Multimedia*, 2024.
- [10] Catalin Ionescu, Dragos Papava, Vlad Olaru, and Cristian Sminchisescu. Human3.6m: Large scale datasets and predictive methods for 3d human sensing in natural environments. *IEEE Transactions on Pattern Analysis and Machine Intelligence*, 36(7):1325–1339, jul 2014.
- [11] Filipa Lino, Carlos Santiago, and Manuel Marques. 3d human pose estimation with occlusions: Introducing blendmimic3d dataset and gcn refinement. In *Proceedings of the IEEE/CVF Conference on Computer Vision and Pattern Recognition*, pages 4646–4656, 2024.
- [12] Tsung-Yi Lin, Michael Maire, Serge Belongie, James Hays, Pietro Perona, Deva Ramanan, Piotr Dollár, and C Lawrence Zitnick. Microsoft coco: Common objects in context. In *Computer vision—ECCV 2014: 13th European conference, zurich, Switzerland, September 6–12, 2014, proceedings, part v 13*, pages 740–755. Springer, 2014.
- [13] Xuke Yan, Bo Liu, and Guangzhi Qu. Efficient monocular human pose estimation based on deep learning methods: A survey. *IEEE Access*, 2024.
- [14] Sijin Li and Antoni B Chan. 3d human pose estimation from monocular images with deep convolutional neural network. In *Asian conference on computer vision*, pages 332–347. Springer, 2014.
- [15] Georgios Pavlakos, Xiaowei Zhou, and Kostas Daniilidis. Ordinal depth supervision for 3d human pose estimation. In *Proceedings of the IEEE conference on computer vision and pattern recognition*, pages 7307–7316, 2018.
- [16] István Sáráandi, Alexander Hermans, and Bastian Leibe. Learning 3d human pose estimation from dozens of datasets using a geometry-aware autoencoder to bridge between skeleton formats. In *Proceedings of the IEEE/CVF Winter Conference on Applications of Computer Vision*, pages 2956–2966, 2023.
- [17] Dario Pavllo, Christoph Feichtenhofer, David Grangier, and Michael Auli. 3d human pose estimation in video with temporal convolutions and semi-supervised training. In *Proceedings of the IEEE/CVF conference on computer vision and pattern recognition*, pages 7753–7762, 2019.
- [18] Zhongwei Qiu, Kai Qiu, Jianlong Fu, and Dongmei Fu. Dgcn: Dynamic graph convolutional network for efficient multi-person pose estimation. In *Proceedings of the AAAI Conference on Artificial Intelligence*, volume 34, pages 11924–11931, 2020.
- [19] Yujun Cai, Lihao Ge, Jun Liu, Jianfei Cai, Tat-Jen Cham, Junsong Yuan, and Nadia Magnenat Thalmann. Exploiting spatial-temporal relationships for 3d pose estimation via graph convolutional networks. In *Proceedings of the IEEE/CVF international conference on computer vision*, pages 2272–2281, 2019.
- [20] Jinlu Zhang, Zhigang Tu, Jianyu Yang, Yujin Chen, and Junsong Yuan. Mixste: Seq2seq mixed spatio-temporal encoder for 3d human pose estimation in video. In *Proceedings of the IEEE/CVF conference on computer vision and pattern recognition*, pages 13232–13242, 2022.
- [21] Qitao Zhao, Ce Zheng, Mengyuan Liu, Pichao Wang, and Chen Chen. Poseformerv2: Exploring frequency domain for efficient and robust 3d human pose estimation. In *Proceedings of the IEEE/CVF conference on computer vision and pattern recognition*, pages 8877–8886, 2023.
- [22] Wenkang Shan, Zhenhua Liu, Xinfeng Zhang, Zhao Wang, Kai Han, Shanshe Wang, Siwei Ma, and Wen Gao. Diffusion-based 3d human pose estimation with multi-hypothesis aggregation. In *Proceedings of the IEEE/CVF International Conference on Computer Vision*, pages 14761–14771, 2023.

- [23] Donghoon Lee and Jaeho Kim. Hdpose: Post-hierarchical diffusion with conditioning for 3d human pose estimation. *Sensors*, 24(3):829, 2024.
- [24] Han Yu, Congju Du, and Li Yu. Scale-aware heatmap representation for human pose estimation. *Pattern Recognition Letters*, 154:1–6, 2022.
- [25] Yu Cheng, Bo Yang, Bo Wang, Wending Yan, and Robby T Tan. Occlusion-aware networks for 3d human pose estimation in video. In *Proceedings of the IEEE/CVF international conference on computer vision*, pages 723–732, 2019.
- [26] Junjie Wang, Zhenbo Yu, Zhengyan Tong, Hang Wang, Jinxian Liu, Wenjun Zhang, and Xiaoyan Wu. Ocr-pose: Occlusion-aware contrastive representation for unsupervised 3d human pose estimation. In *Proceedings of the 30th ACM International Conference on Multimedia*, pages 5477–5485, 2022.
- [27] Peter Hardy and Hansung Kim. Links" lifting independent keypoints"-partial pose lifting for occlusion handling with improved accuracy in 2d-3d human pose estimation. In *Proceedings of the IEEE/CVF Winter Conference on Applications of Computer Vision*, pages 3426–3435, 2024.
- [28] Michał Rapczyński, Philipp Werner, Sebastian Handrich, and Ayoub Al-Hamadi. A baseline for cross-database 3d human pose estimation. *Sensors*, 21(11):3769, 2021.
- [29] Naureen Mahmood, Nima Ghorbani, Nikolaus F Troje, Gerard Pons-Moll, and Michael J Black. Amass: Archive of motion capture as surface shapes. In *Proceedings of the IEEE/CVF international conference on computer vision*, pages 5442–5451, 2019.
- [30] Matthew Loper, Naureen Mahmood, Javier Romero, Gerard Pons-Moll, and Michael J Black. Smpl: A skinned multi-person linear model. In *Seminal Graphics Papers: Pushing the Boundaries, Volume 2*, pages 851–866. 2023.
- [31] Yilun Chen, Zhicheng Wang, Yuxiang Peng, Zhiqiang Zhang, Gang Yu, and Jian Sun. Cascaded pyramid network for multi-person pose estimation. In *Proceedings of the IEEE conference on computer vision and pattern recognition*, pages 7103–7112, 2018.
- [32] Yuxin Wu, Alexander Kirillov, Francisco Massa, Wan-Yen Lo, and Ross Girshick. Detectron2: A pytorch-based modular object detection library. *Meta AI*, 10:2, 2019.